Surface stresses in paraffin and polyethylene*

H. P. Fisher and R. K. Eby†
Department and Institute of Polymer Science, The University of Akron, Akron, OH 44325, USA

and R. C. Cammarata
Department of Materials Science and Engineering, The Johns Hopkins University, Baltimore, MD 21218, USA
(Received 15 December 1993; revised 16 January 1994)

Previous calculations of surface stress in polyethylene and paraffin crystals are extended to include other experimental and computational data. There are significant changes in the magnitude of the stresses. For polyethylene, these might reflect variations in the nature of the fold surface. Computational modelling yields surface stresses and energies that agree with the experimentally based magnitudes for paraffins but disagree with those for polyethylene. The discrepancy is not reduced by taking account of the effect of neighbouring crystals in the modelling. The agreement of the paraffin modelling results with experiment suggests that the discrepancy for polyethylene has its origins in the model of the fold surface. This raises the possibility that modelling can be used to investigate the nature of the fold surface.

(Keywords: surface stress; paraffin; polyethylene)

INTRODUCTION

Associated with the interface or surface of a crystalline material are a surface energy and a surface stress. The former is the reversible work required to create a new surface of unit area by a process such as cleavage and the latter is the reversible work required to create a unit area of surface by deformation of a pre-existing surface. The stress can result from missing neighbouring atoms at an interface or surface, different atoms or chemical groups, and physically different structures such as molecular folds. It has been shown previously that surface stress can cause both the lattice strain and the elastic behaviour of multilayered thin metallic films[1]. Surface stress in polymer crystals can play a role in properties and morphological features such as twisted lamellae, curved crystals, ridged lamellae, S-shaped lamellar crystals, anisotropic strain of the unit cells, strain energy of the crystals, melting temperature, specific heat, density, and the elastic behaviour[2-11].

The surface stress has been analysed for thin lamellar crystals of polymers and paraffins. In the case of orthorhombic crystals with the molecules perpendicular to the surface, surface stress in the a and b dimensions, f_a and f_b, can be expressed as[12]:

$$f_a = -l(S_{22}\varepsilon_a - S_{12}\varepsilon_b)/[2(S_{11}S_{22} - S_{12}^2)] \quad (1)$$

$$f_b = -l(-S_{12}\varepsilon_a + S_{11}\varepsilon_b)/[2(S_{11}S_{22} - S_{12}^2)] \quad (2)$$

In these equations, l is the lamella thickness, ε_a and ε_b are the experimentally derived strains in the a and b crystallographic directions, respectively, and the subscripts to the S terms denote the computed elastic compliances expressed in the simplified notation. Equations (1) and (2) have been used to calculate surface stresses for n-paraffins and polyethylene[12]. This paper extends those calculations for the paraffins and polyethylene to incorporate other experimentally derived strains and other computed elastic compliances. It also demonstrates the use of computer modelling of surface stress to investigate the nature of crystal surfaces for those two materials. Epitaxy is also examined briefly.

STRAINS AND COMPLIANCES

In a series of experimental investigations the changes in the unit cell and lamella thickness for both n-paraffins[13] and polyethylene[9,13,14] were examined by X-ray diffraction. Crystals were obtained through either melt or solution crystallization and the changes in the crystallographic dimensions of the unit cell were measured as a function of temperature and lamella thickness. These results can be expressed as strains in the a and b axes. (Note that the strain in ref. 12 contains the inverse of the crystal thickness.) Some of the results from the experiments are summarized in *Table 1*.

The data from ref. 13 for paraffins and ref. 9 for polyethylene were used in the calculations for ref. 12. The negative strain for b in ref. 9 is not in agreement with most other experimental results and remains unexplained. A negative strain has also been observed for a in paraffins at a lower temperature[13].

* Presented at 'International Polymer Physics Symposium Honouring Professor John D. Hoffman's 70th Birthday', 15–16 May 1993, Washington, DC, USA
† To whom correspondence should be addressed

0032-3861/94/09/1923–08

Experimental elastic compliances for the determination of surface stress by equations (1) and (2) are not available. A number of researchers have calculated compliances for paraffinic crystals[15–20]. The results vary with setting angle and, therefore, have been interpolated to the setting angles found for paraffin and polyethylene in the computer models to be discussed in the Results and Discussion section below. As noted there, these angles are similar to the experimental ones. The results of the interpolation are given in *Table 2*.

In ref. 12, the experimental strains of refs 9 and 13 and the computed elastic compliances of ref. 20 were combined in equations (1) and (2) to yield the hybrid surface stress magnitudes for n-paraffins and polyethylene shown in *Table 3*. These results may be compared with those obtained from data in *Tables 1* and *2* and given in *Table 4*. While the order of magnitude of the stresses did not change, the use of various experimental strains and the improved values for the calculated compliances did produce some significant changes. Those associated with the variations in strain for polyethylene might reflect variations in the nature of the fold surface. Note also that the stresses based on refs 13 and 14 for polyethylene are now greater than the stresses for the paraffins. This intuitively expected relationship will be revisited later.

COMPUTATIONAL METHODS

Computational modelling was done using the Sybyl 5.5[21] modelling software and the associated Tripos[22] force field. The paraffin crystal was modelled with 14 stems in an orthorhombic unit cell and perpendicular to the crystal surface, corresponding to the analysis used in ref. 12. The arrangement is shown in *Figure 1*. Each stem comprised 40 carbon atoms and the associated hydrogen atoms for a total of 1708 atoms explicitly modelled by the system. This number was found to be near the optimal compromise in terms of usefully realistic results, computational efficiency, and computer hardware ability. *Table 5* shows the default modelling parameters that were used.

A useful model ought to reproduce adequately the experimental values of the unit cell parameters and the surface energy. Therefore, these results were determined first. The crystallographic parameters of the minimum energy orthorhombic unit cell were determined by a grid search in 0.05 Å steps in a and b together with 1° steps in the setting angle, θ, of the carbon backbone with respect to the b axis. These values were reduced in steps to 0.002 Å and 0.5° near the minimum. The energy associated with the atoms in the defined surface region of this unit cell was also calculated. The excess surface energy is associated with the difference between the energy of a number of atoms at the surface of the central stem pair and the energy of the same number of atoms on the stem pair in the centre of the crystal. When this difference

Table 1 Strains derived from experimental determinations of the unit cell

Material	Ref.	$\varepsilon_a(\times 10^{-11}/l)$ (m^{-1})	$\varepsilon_b(\times 10^{-11}/l)$ (m^{-1})	T (K)
Paraffin	13	2.73	1.32	296.2
Polyethylene	13	5.21	1.43	296.2
Polyethylene	14	5.89	4.54	300
Polyethylene	9	3.54	−0.715	300

Table 3 Surface stress results from ref. 12

Material	Ref.	f_a ($J\,m^{-2}$)	f_b ($J\,m^{-2}$)
Paraffin	13	−0.236	−0.182
Polyethylene	9	−0.212	−0.084

Table 4 Surface stress calculated with data in *Tables 1* and *2*

Material	Ref.	f_a ($J\,m^{-2}$)	f_b ($J\,m^{-2}$)
Paraffin	13	−0.130	−0.087
Polyethylene	13	−0.237	−0.139
Polyethylene	14	−0.322	−0.247
Polyethylene	9	−0.130	−0.043

Table 5 Tripos default parameters used in the modelling calculations

C–C–C bond angle	111.4°
H–C–C bond angle	109.5°
H–C–H bond angle	109.5°
C–C bond length	1.54 Å
C–H bond length	1.10 Å

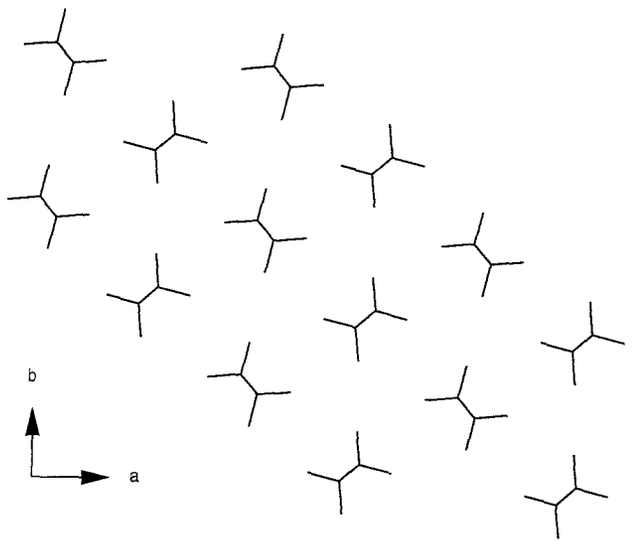

Figure 1 The orthorhombic unit cells of the 40 carbon paraffin model viewed along the c axis

Table 2 Calculated elastic compliances for selected setting angles

Material	Setting angle (deg)	S_{11} ($\times 10^{-12}\,Pa^{-1}$)	S_{12} ($\times 10^{-12}\,Pa^{-1}$)	S_{22} ($\times 10^{-12}\,Pa^{-1}$)
Paraffin	44.5	182	−114	246
Polyethylene	46.0	204	−153	303

becomes independent of the number of atoms, it is the excess energy of the surface with respect to the crystal.

Differences, ΔE, in the excess energy of the surface with respect to the crystal between adjacent grid points in the a and b crystallographic directions around the unit cell of minimum energy allow the surface stresses to be determined through the following equations:

$$f_a = (\Delta E/\Delta a)_b/b \quad (3)$$

$$f_b = (\Delta E/\Delta b)_a/a \quad (4)$$

Results from these calculations will be compared with the hybrid results of surface stress in *Table 4*.

In order to model the chain-folded polyethylene lamella, a number of changes had to be made. The size of the modelled system remained consistent with the previous paraffin model. It comprised seven identical fold and stem pairs containing 80 carbon atoms, and the associated hydrogen atoms approximately one-half of a polyethylene lamella. These were placed into an orthorhombic array with the stems perpendicular to the fold surface and the folds along the 110 direction lined up in the a and b directions[23]. There are, of course, many other models of the folds and fold surface. The model used is one of the simpler to use in an initial study. The arrangement is shown in *Figure 2*.

As a starting point, the previously determined isolated fold of 12 carbon atoms was used[24]. It is similar in conformation to isolated folds found by others[25,26]. Other folds were generated by using a modified Metropolis algorithm and simulated annealing methods[27]. From the starting conformation, the central fold energy was minimized, with the atomic positions of all the stems and other folds held fixed. The resulting conformation of the central fold was used to replace the conformations of the exterior folds while the stems remained unchanged. This iterative process continued until the energy of the last model was approximately equal to the energy of the previous model. These steps were repeated in conjunction with a grid search in a, b and θ. The minimized unit cell for each a and b pair was taken as the system that resulted in the lowest total intra- and intermolecular energy associated with the atoms in the central fold and stem pair. As a further check, the fold corresponding to the global minimum was used as a starting conformation for the surrounding unit cells in the grid. If one of these yielded a lower energy, the process was repeated until no change was found. This final cell was taken as the minimum.

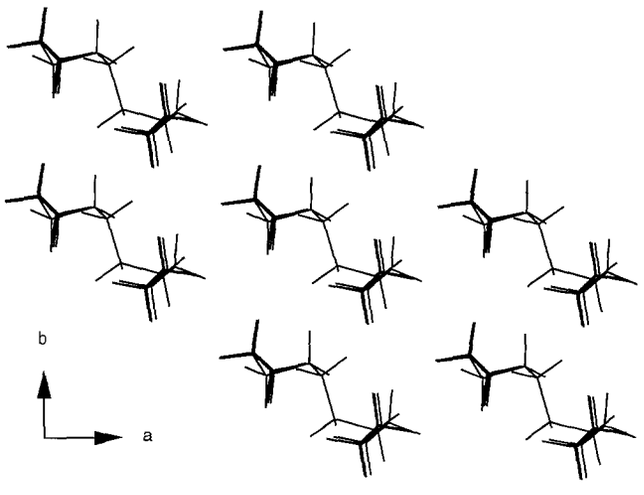

Figure 2 The orthorhombic unit cell of the 80 carbon polyethylene model viewed along the c axis

Table 6 Experimental and calculated unit cell parameters for n-paraffins

Ref.	Chain size	Unit cell parameters		
		a (Å)	b (Å)	θ (deg)
Experimental				
28	C25	7.45	4.95	43
28	C27	7.48	4.97	42
28	C30	7.44	4.96	44
28	C32	7.44	4.95	43
28	C35	7.43	4.91	47
28	C94	7.43	4.92	45
Modelling				
29	–	7.26	4.94	42
30	C8	7.26	4.94	42
31	C20	7.23	4.94	42
This study	C40	7.330	5.118	44.5

The number of carbon atoms to be minimized in the fold was re-examined during the investigations by determining the excess surface energy with respect to the crystal. The number of carbon atoms that determined the excess was taken as the number of carbon atoms associated with the fold. Calculations were also carried out for the energy of an isolated fold–stem pair as a function of the unit cell parameters and the number of atoms taken as the fold, in a similar manner to that used before[24]. Finally, the number of atoms in the fold of the central fold–stem pair with the minimum energy was examined. The unit cell parameters were held constant while the energy of the isolated fold–stem pair was minimized as a function of the number of atoms in the fold.

RESULTS AND DISCUSSION

Paraffins

The unit cell parameters of n-paraffins of different lengths have been determined experimentally[28]. These results at room temperature are compared with modelled results in *Table 6*. In *Table 6*, the results from ref. 29 represent the unit cell parameters of bulk polyethylene without reference to a crystal surface. Also, the results in refs 30 and 31 were obtained with a CH_2 group on the ends of the molecules. A contour plot of the change in the a and b dimensions as a function of the energy of the central stem pair is shown in *Figure 3*. These data yield the last row of results in *Table 6*. They are in reasonable agreement with the other results from modelling and experiment. Variations in the modelling probably arise from differences among the force fields, default parameters and minimization procedures used.

In *Figure 4*, curve A shows the difference between the energy of carbon and associated hydrogen atoms in the surface and in the interior of the crystal for the lowest energy central stem pair as a function of the number of carbon atoms considered. These indicate a surface region to which carbon atoms about four deep in each stem contribute decreasingly with depth. The excess surface energy with respect to the crystal is about 21.3 kJ mol^{-1} (5.1 kcal mol^{-1}) of two surface methyl groups. To reduce the effects of small variations in the minimized energy,

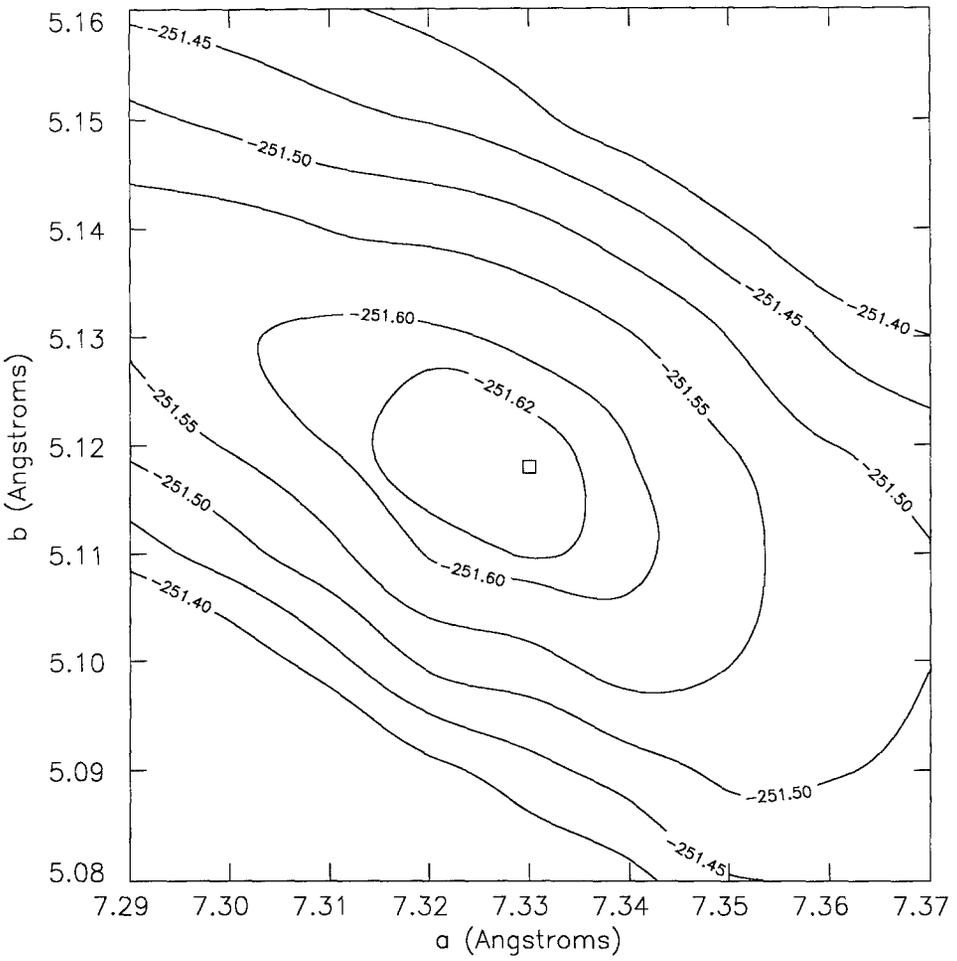

Figure 3 Energy of the central stem pair for the 40 carbon paraffin model as a function of the a and b dimensions of the unit cell. Note that the setting angle also varies over the range of dimensions. Since the minimum is shallow, very small variations in energy lead to irregularities in the lines of constant energy

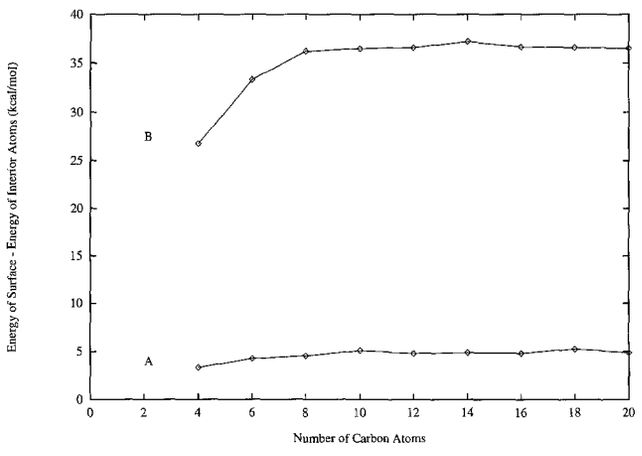

Figure 4 A, Difference between the energy of carbon and associated hydrogen atoms on the surface and in the interior of the paraffin model as a function of the number of carbon atoms in two stems. The data are for the lowest energy stem pair in the centre of the model. B, Difference between the energy of carbon and associated hydrogen atoms on the fold surface and in the interior of the chain-folded polyethylene model as a function of the number of carbon atoms in the fold. The data are for the lowest energy fold–stem pair in the centre of the model

the energies of the surface corresponding to 121 grid points about the minimum were fitted to a polynomial in a and b. The polynomial was used to determine the energies for the subsequent analyses. This procedure changed the results by only a minor amount from those obtained with the original data. (The unfitted data are presented in the figures in order to show typical scatter.)

The surface energy with reference to the melt state is frequently determined experimentally by melting temperature measurements. The excess energy with respect to the crystal can be referenced to the melt by the equation:

$$\sigma_e = [E - n(\Delta H_f - T\Delta S_f)]/A \quad (5)$$

where E is the excess energy of the surface with respect to the crystal, ΔH_f is the crystal heat of fusion[32] (4.11 kJ(mol CH_2)$^{-1}$), ΔS_f is the crystal entropy of melting[33] (9.91 J(mol CH_2)$^{-1}$ K^{-1}), A is the basal area of the unit cell, corresponding to the energy minimum, and $n=2$, corresponding to the two surface groups. The conversion term is $<2\%$ of E and could be neglected. (It is $<1\%$ for polyethylene.) Note that the conversion term involves entropy which has not been calculated explicitly for E. There is an implicit entropy effect in the force fields, but it is not matched to the temperatures of interest. In any event, the entropies of the crystal and surface are probably not too large. The equation yields a surface energy of 0.085 J m^{-2} (85 erg cm^{-2}). The calculated result can be compared with the experimentally determined value of 0.100–0.112 J m^{-2} (100–112 erg cm^{-2})[33,34].

Surface stress can be calculated by using equations (3) and (4) together with the unit cell dimensions and the

excess surface energy with respect to the crystal, as determined by the polynomial discussed above. The results shown in *Table 7* indicate good agreement between the hybrid (*Table 4*) and computational methods of determining surface stress for the paraffin.

Polyethylene

A contour plot of the minimized energy of the central 80 carbon fold–stem pair is shown in *Figure 5*. The low energy parameters, along with different modelling and experimental results (from various sources, including refs 35–37), are given in *Table 8*. The minimized unit cell results from this study are in general agreement with previous modelling and experimental results. Again, variations in the results of modelling arise from differences among the force fields, default parameters, minimization procedures and (for polyethylene) fold models used. The results from this study are also in agreement with experiment in that the modelled dimension *a* for the paraffin exceeds that for polyethylene by an amount comparable to the average experimental difference. Further, the two corresponding differences for *b* are both very close to zero.

Table 7 Modelled surface stresses for a paraffin crystal

f_a (J m^{-2})	f_b (J m^{-2})
−0.130	−0.053

Adjacent re-entry folds at a crystal surface have been experimentally studied for a triclinic cyclic paraffin[38] in which the 'stems' are almost perpendicular to the fold surface. This work showed the presence of four approximately *gauche* torsion angles in an adjacent re-entry fold with a length not too different from the length found for polyethylene. It also demonstrated the importance of bond angles in contributing to the surface energy. Comparison of the fold conformations from the present and other modelling studies reveals minor differences among the results[25,26]. However, the overall conformations are similar and all exhibit five approximately *gauche* torsion angles. These results are presented in *Table 9* together with the bond angles. The folds generated by other methods during the present analysis were not too different from the one given in the table, but were somewhat greater in energy (<3 to >10 kcal mol^{-1}).

The surface energy of a polyethylene crystal was estimated in early studies by the energy required to fold a chain back upon itself[39]. The estimate assumed that a fold comprised five *gauche* torsion angles, an idea that is in agreement with the models above. Based upon the energy associated with a *gauche* torsion, it was predicted that the surface energy would be in

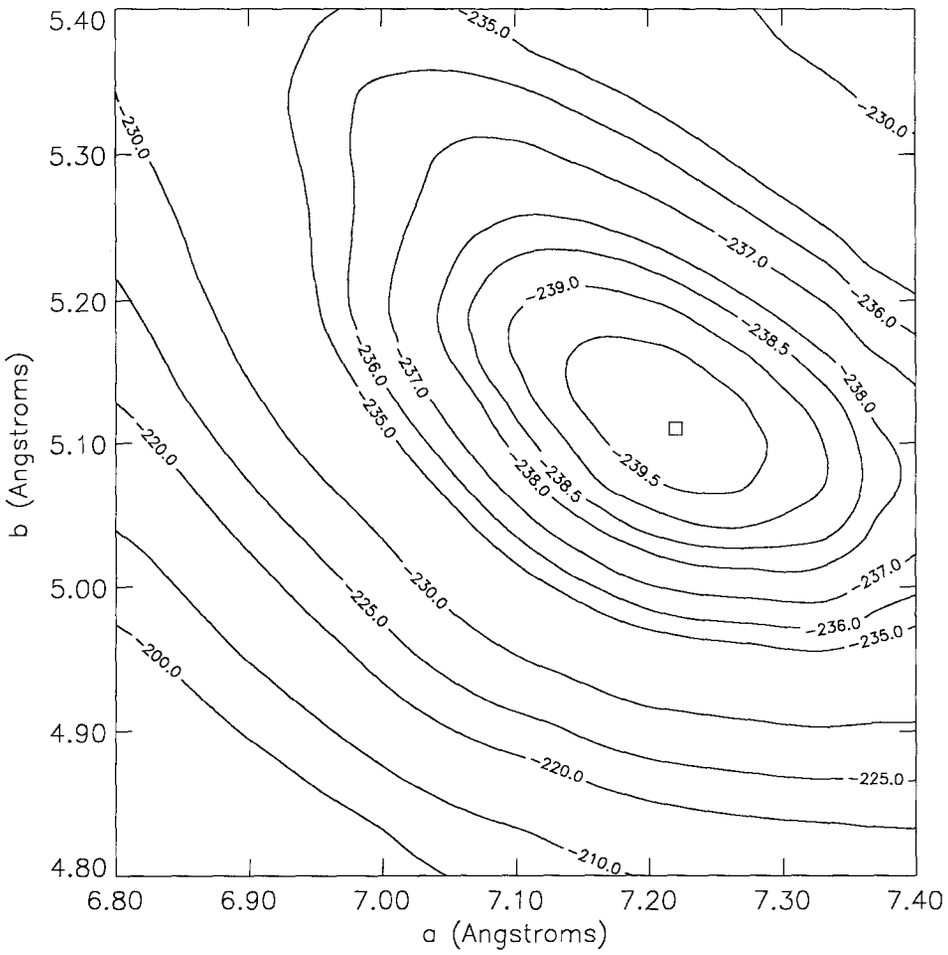

Figure 5 Energy of the central fold–stem pair for the 80 carbon polyethylene model as a function of the *a* and *b* dimensions of the unit cell. Note that the setting angle also varies over the range of dimensions. Since the minimum is shallow, very small variations in energy lead to irregularities in the lines of constant energy

Table 8 Experimental and modelled unit cells for polyethylene

Ref.	*a* (Å)	*b* (Å)	*θ* (deg)
Experimental			
9	7.397	4.935	–
15	7.399	4.945	–
35	7.414	4.942	–
36	7.388	4.929	45
Modelling			
8	7.10	4.905	48
26	7.2	5.0	46
37	7.4	4.93	41
This study	7.23	5.114	46

Table 9 Comparison of the torsion and bond angles in the fold for different models

	Ref. 25	Ref. 26	This study
Torsion angle (deg)			
1	74.8	77.2	72.3
2	174.8	182.0	167.2
3	68.4	66.7	80.8
4	91.6	87.9	74.2
5	−58.4	−65.5	−55.2
6	−64.4	−62.1	−60.8
7	174.4	182.9	175.0
Bond angle (deg)			
1	113.6	114.44	113.82
2	112.7	113.27	111.52
3	114.8	115.50	115.20
4	114.8	116.74	115.45
5	116.2	116.45	116.76
6	114.0	117.12	121.84

Table 10 Modelling results for the surface stress in polyethylene

f_a ($J\,m^{-2}$)	f_b ($J\,m^{-2}$)
−2.180	−2.840

the range of 0.057–0.085 $J\,m^{-2}$ (57–85 $erg\,cm^{-2}$). Most of the experimental values determined by melting point analysis have ranged from 0.075 to 0.095 $J\,m^{-2}$ (75–95 $erg\,cm^{-2}$)[32,40].

The surface region of the final polyethylene model comprises eight carbon atoms associated with the central fold. This number is based upon curve B of *Figure 4*, which shows the difference between the energy of the carbon atoms and the associated hydrogen atoms on the surface and in the interior as a function of the number of carbon atoms. The excess surface energy with respect to the melt can be determined by the use of equation (5) and the excess energy of the surface with respect to the crystal of 151.5 $kJ\,mol^{-1}$ (36.2 $kcal\,mol^{-1}$) from the polynomial discussed above. This results in a value of 0.643 $J\,m^{-2}$ (643 $erg\,cm^{-2}$) for the excess surface energy with respect to the melt of the minimized polyethylene unit cell, a result in marked disagreement with the much smaller experimental values. It is also much greater than the energies calculated for isolated fold and stem pairs[24–26,39]. Most of the extra energy arises from bond angle bending and the increased van der Waals energy for the fold in comparison to the stem atoms in the interior of the crystal.

Finally, the values of surface stress in the *a* and *b* crystallographic directions can be determined from the change of excess surface energy with respect to the crystal through the use of equations (3) and (4). The results presented in *Table 10* can be compared to the hybrid results given in *Table 4*. These results for the surface stress based upon a pure modelling approach are also much greater in magnitude than the results calculated through the hybrid approach. The former are probably incorrect since the surface stresses determined by the hybrid models are of the order of the surface energy expected for chain-folded polyethylene[12].

The crystals for which the experimental strains were determined had been grown under a variety of conditions, noted earlier. For all of these, there is some degree of interaction between neighbouring crystals. This could range from weaker to stronger, depending upon the extent of contact, orientation, regularity of the fold surface, etc. However, implicit in the present analysis and models is the assumption that the surface stress for a free-standing crystal is approximately the same as that between neighbouring crystals. This assumption is not completely valid, since the neighbouring crystals will affect the magnitude of the excess surface energy. This would be especially so for the polyethylene model, since the folds extend above the crystal in such a manner that periodically located depressions are created among them. Thus, the consequence would be not only missing favourable interactions from missing neighbours above the fold surface but also reduced favourable interaction laterally within the surface.

To make an initial assessment of the magnitude of these effects, the docking program in the Sybyl[21] software was used to bring the model in *Figure 2* into opposition to another fold surface. The program allows the movable surface to be arranged parallel to the other and to be translated/rotated within the parallel plane. Also, the perpendicular separation between the two surfaces can be changed. These parameters were varied until the energy of the system was minimized.

The resulting juxtaposition of the two arrays is shown in *Figure 6*, in which the folds of one array are positioned over the depressions of the other. There are related epitaxial arrangements of similar energy. The one in *Figure 6* was achieved by bringing identical fold surfaces into opposition. It differs from other possible packing modes that have been discussed as illustrative[41] and can be made by bringing into opposition two fold surfaces which are mirror images. The excess energy with respect to the crystal of the fold from the low energy central fold–stem pair has now been reduced to 124.3 $kJ\,mol^{-1}$ (29.7 $kcal\,mol^{-1}$). This reduces the excess energy of the surface with respect to the melt to 0.52 $J\,m^{-2}$ (520 $erg\,cm^{-2}$). Finally, the surface stresses have been reduced to $-1.29\,J\,m^{-2}$ in the *a* direction and $-2.33\,J\,m^{-2}$ in the *b* direction. Thus, the effects are not large enough to resolve the discrepancies with respect to the magnitude of the experimental excess surface energy and the hybrid surface stresses. For the reasons discussed above, the effects for the folds are expected to be relatively larger than those for the paraffins.

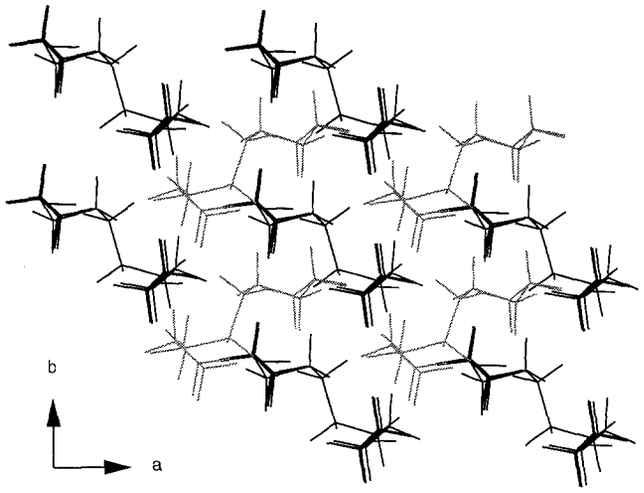

Figure 6 Juxtaposition of two crystals with opposed surfaces (light and dark) after docking to minimize the energy of the system. The energy of the central fold–stem pair in the light array is used for the subsequent analysis

SUMMARY AND CONCLUSION

The model predicts the excess surface energy with respect to the melt and the surface stress for the paraffin with reasonable accuracy, but the polyethylene model seriously overestimates the magnitude of these quantities. The overestimation is reduced, but not eliminated, by taking account of interactions between neighbouring crystals. It is possible that the overestimation results from errors in the nature of the fold surface used, since this is the obvious difference between the two cases. It is also possible that the force field might not yield results for strained molecules and close contacts that are as valid as those for 'equilibrium' situations. Such strains and close contacts occur in the fold surface. The force field also includes the consequences of molecular vibrations. Therefore, there is an implied temperature dependence. As a consequence, the temperatures for which the excess energy of the surface with respect to the melt and the surface stresses were evaluated experimentally should be matched by the temperature for which the force field is most valid. This, of course, is not the case. However, estimations of the temperature effect suggest that this error is not too large, a result supported by the relative success of the modelling for the paraffins.

There are possible conformational entropy and internal energy effects associated with the folds. Those folds considered in the model were generated with the stems held fixed, but those formed during crystallization are subject to less severe restrictions. Thus, a real crystal might exhibit more variations in the fold surface with associated effects on free energy. This allows consideration of less regular folds, cilia, asymmetrical folds with one stem higher than the other (staggered folds)[42], etc.

Other possible variations in the model that might affect the surface energy involve the overall fold surface itself. For example, the folds in the 110 direction might be arrayed along the 110 direction rather than along *a* and *b* as in the present model. Further, the folds themselves might be made in the *b* direction. Tilted fold surfaces that are not perpendicular to the stems also should be considered. This case also would require a revision of the elastic analysis used to calculate the surface stress with experimental data, since that analysis assumed the stems to be perpendicular to the fold surface[12]. This modification might increase the hybrid stresses for polyethylene with respect to the paraffins. It might also bring the hybrid stresses into better agreement with the results of modelling. In any event, it seems probable that the discrepancy arises from deficiencies in the modelling of the folds and/or fold surface.

These results illustrate the potential use of computer modelling of surface stresses and surface energy to investigate the nature of the folds and fold surface.

ACKNOWLEDGEMENTS

This work was supported in part by the Robert C. Musson Charitable Trust and Tripos Associates, Inc. Helpful discussions with Professor B. L. Farmer and K. S. Macturk are gratefully acknowledged.

REFERENCES

1 Cammarata, R. C. and Sieradzki, K. *Phys. Rev. Lett.* 1989, **62**, 2005
2 Bassett, D. C. 'Principles of Polymer Morphology', Cambridge University Press, Cambridge, 1981
3 Keith, H. D., Padden, F. J. Jr, Lotz, B. and Wittman, J. C. *Macromolecules* 1989, **22**, 2230; Keith, H. D. and Padden, F. J. Jr. *Polymer* 1984, **25**, 28
4 Khoury, F. H. and Barnes, J. D. *J. Res. Nat. Bur. Std* 1972, **76A**, 225
5 Bassett, D. C. *Phil. Mag.* 1964, **10**, 595
6 Hoffman, J. D. and Lauritzen, J. I. Jr *J. Res. Nat. Bur. Std* 1961, **65A**, 297; Hoffman, J. D. and Miller, R. L. *Macromolecules* 1989, **22**, 3038
7 Okano, K. *Jpn J. Appl. Phys.* 1964, **3**, 351
8 Marand, H. *Macromolecules* 1989, **22**, 3980
9 Davis, G. T., Eby, R. K. and Colson, J. P. *J. Appl. Phys.* 1970, **41**, 4316
10 Howard, P. R. and Christ, B. *J. Polym. Sci.* 1989, **B27**, 2269
11 Bunn, C. W. in 'Polythene' (Eds A. Renfrew and P. Morgan), Interscience, New York, 1957, Ch. 7
12 Cammarata, R. C. and Eby, R. K. *J. Mater. Res.* 1991, **6**, 888
13 Davis, G. T., Weeks, J. J., Martin, G. M. and Eby, R. K. *J. Appl. Phys.* 1974, **45**, 4175
14 Davis, G. T., Eby, R. K. and Martin, G. M. *J. Appl. Phys.* 1968, **39**, 4973
15 Kobayashi, M. *J. Chem. Phys.* 1979, **70**, 509
16 Kitagawa, T. and Miyazawa, T. in 'Advances in Polymer Science', Springer-Verlag, Berlin, 1972, Vol. 9, p. 315
17 Odajima, A. and Maeda, T. *J. Polym. Sci.* 1966, **C15**, 55
18 Sorenson, R. A., Liau, W. B., Kesner, L. and Boyd, R. H. *Macromolecules* 1988, **21**, 200
19 Tashiro, K., Kobayashi, M. and Tadokoro, H. *Macromolecules* 1978, **11**, 914
20 Wobser, G. and Blasenbrey, S. *Kolloid Z. Z. Polym.* 1970, **241**, 985
21 Sybyl Molecular Modeling Software Version 5.5, Tripos Associates, Inc., St Louis, MO
22 Clark, M., Cramer R. D. III and Van Opdenbosch, N. *J. Comp. Chem.* 1989, **10**, 982
23 Renecker, D. H. and Geil, P. H. *J. Appl. Phys.* 1960, **31**, 1916
24 Fisher, H. P., Eby, R. K. and Cammarata, R. C. in 'Tech Papers XXXVIII', Society of Plastic Engineers, Brookfield, CT, 1992, p. 1979
25 Petraccone, V., Allegra, G. and Corradini, P. *J. Polym. Sci.* 1972, **C38**, 419
26 Davé, R. S. and Farmer, B. L. *Polymer* 1988, **29**, 1544
27 Press, W. H., Flannery, B. P., Teukolsky, S. A. and Vetterling, W. T. 'Numerical Recipies in C', Cambridge University Press, New York, 1990
28 Kawaguchi, A., Ohara, M. and Kobayashi, K. *J. Macromol. Sci.-Phys.* 1979, **B8**, 193
29 Boyd, R. H. *J. Polym. Sci., Polym. Phys. Edn.* 1975, **13**, 2345
30 Farmer, B. L. and Eby, R. K. *J. Appl. Phys.* 1975, **46**, 4209

31 Farmer, B. L. and Eby, R. K. *Polymer* 1979, **20**, 363
32 Wunderlich, B. and Czornyj, G. *Macromolecules* 1977, **10**, 907
33 Wunderlich, B. 'Macromolecular Physics', Academic Press, New York, 1980, Vol. 3
34 Broadhurst, M. G. *J. Chem. Phys.* 1962, **36**, 2578
35 Swan, P. R. *J. Polym. Sci.* 1962, **56**, 403
36 Kavesh, S. and Schultz, J. M. *J. Polym. Sci.* 1970, **A2**, 243
37 Oyama, M., Shiokawa, K. and Ishimaru, T. *J. Macromol. Sci. Phys.* 1973, **B8**, 229
38 Kay, H. F. and Newman, B. A. *J. Appl. Phys.* 1967, **38**, 4105; Grossman, H. P., Arnold, R. and Bürkle, K. R. *Polym. Bull.* 1980, **3**, 135; Lee, K.-S., Wegner, G. and Hsu, S. L. *Polymer* 1987, **28**, 889
39 Hoffman, J. D. *SPE Trans.* 1964, 315
40 Illers, K. H. and Hendus, H. *Makromol. Chem.* 1968, **113**, 1
41 Holland, V. F. and Lindenmeyer, P. H. *J. Appl. Phys.* 1965, **36**, 3049
42 Mazur, J., Khoury, F. and Fanconi, B. *Bull Am. Phys. Soc.* 1983, **28**, 393